A Refined Model for Predicting the 31-Coupling Effect of Piezoelectric Structural Fiber Composites

Yaoling Xu and Lishuang Zheng

Key Laboratory of Mechanical Reliability for Heavy Equipments and Large Structures of Hebei Province, Yanshan University, Qinhuangdao, China.
Email: xylysu@163.com

Abstract. A refined model is proposed to predict the 31-coupling effect of a piezoelectric structural fiber (PSF) and PSF composites. The PSF model consists of a piezoelectric shell, inner and outer electrode layers, and a piezoelectric inactive core fiber. The inner and outer electrodes provide a radial electric field passing through the piezoelectric shell, which leads to the axial deformation of the piezoelectric shell, the piezoelectric inactive core fiber provides the mechanical support to the brittle piezoelectric shell. Analytical expressions of the effective piezoelectric coefficient d_{31} of the single PSF and the PSF composites are derived, the influences of aspect ratio of the piezoelectric shell, thickness of the electrode layer and PSF volume fraction, on the effective piezoelectric coefficient d_{31} are demonstrated. The numerical results show that the model without electrode layers may lead to a significant error.

1. Introduction

The piezoelectric materials have been widely used in sensing and actuation [1-4], fragile nature of the monolithic piezoelectric materials limits their applications in many situations, so the piezoelectric fiber composites have been developed, in which the polymer matrix can provide improved robustness by protecting the fragile fibers and allow the composites to more easily conform to the curved surfaces found in more realistic industrial applications. A common form of piezoelectric fiber composites is based on embedded solid piezoelectric fibers activated by an external interdigitated electrode pattern. Although this type of composite is very useful for anisotropic activation of composites, it requires the electric field to pass through the composite matrix (the electrodes are placed on the matrix surface), which leads to the requirement of high voltages for actuation due to significant electric field losses. Additionally, this type of composite is constrained to non-conductive matrix materials and constructed usually in the form of a patch of material which can be bonded to the surface of a structure or laid-up as active layers along with conventional fiber-reinforced composites, and it is still generally separate from the structural components and not intended to provide any load bearing functionality [5].

In order to overcome the drawbacks of the solid piezoelectric fiber composites, the hollow piezoelectric fiber composite was proposed [6-8], and the feasibility of producing hollow piezoelectric fiber has been investigated [9]. In the hollow piezoelectric fiber composite, the hollow piezoelectric fibers are individually electroded on both the inside and outside surfaces of the hollow fibers, and activated by an electric field applied directly across the wall of the hollow fiber, which generate longitudinal strain due to the piezoelectric coefficient d_{31}. Even though the longitudinal strain of the hollow piezoelectric fiber composite is decreased by approximately half by using d_{31} versus the d_{33} mode used in solid piezoelectric fiber composites, the required voltage can be decreased by a factor of ten or more since the electric field is applied only across the wall of the hollow piezoelectric fiber instead of through the matrix, thereby electric field losses are eliminated. Moreover, the hollow

piezoelectric fibers isolate the inner electrode from the matrix, which enable the fiber to be embedded in electrically conductive matrices.

However, hollow fibers are prone to cracking and failure under mechanical loading due to the fragile nature of the fiber walls. Recently, the piezoelectric structural fiber (PSF), which consists of a piezoelectric inactive core fiber coated with a piezoelectric material, has been developed [10], the piezoelectric inactive core fiber provides the mechanical support to the brittle piezoelectric shell and carries part of the mechanical loading, an electrical potential difference between the inner and outer electrodes gives rise to an electrical polarization and an actuating electric field in the radial direction of the piezoelectric shell, corresponding axial deformation of the fiber is induced by the 31-coupling effect of the piezoelectric materials. The piezoelectric inactive core can be nonconductive materials such as glass [11] or conductive materials such as metals [12, 13], Carbon and Silicon Carbonate [14]. The conductive core can serve as an electrode, while for nonconductive cores, an inner electrode must be placed between the core fiber and the piezoelectric shell.

The single PSF and PSF composites in which PSFs are deployed unidirectionally into the polymer matrix have many practical applications in sensing and actuating, the effective piezoelectric coefficients are key parameters of the PSF and the PSF composites. Brei and Cannon [8] evaluated the effective d_{31} of the hollow piezoelectric fiber and hollow piezoelectric fiber composites, and investigated the effects of the key design parameters (matrix/fiber Young's moduli, aspect ratio of the individual fibers, and the overall active composite volume fraction) on the performance, manufacturing and reliability of the hollow piezoelectric fiber and hollow piezoelectric fiber composites. Beckert et al. [11] predicted effective properties of PSF composites with the glass core by three different methods (finite element method, effective field method, and homogeneous filed approach). Lin and Sodano [5, 14] developed a one-dimensional micromechanics model to obtain the effective d_{31} of the PSF and the PSF composites.

In the works mentioned above, the electrode layers are neglected in the models due to its small thickness. In some cases, the electrode layer should be considered in the models based on the following reasons: (1) very thin electrode layers are prone to damage, which will leads to the failures of the PSF fiber and the PSF composites due to losing electric connectivity, so a thick electrode layer is beneficial to maintain the integrity of the electrode; (2) hollow piezoelectric fibers can be fabricated in very small sizes, even the wall thickness of the hollow piezoelectric fiber maybe on the order of a grain size. Compared with the wall thickness, the electrode layer cannot be neglected in size; (3) the stiffness of the metal (typical platinum and wolfram) is usually several times larger than that of the piezoelectric ceramics, so significant errors may occur due to neglecting the electrode layer in the model. This paper proposes a refined PSF model, in which inner and outer electrode layers are considered. Analytical expressions of the effective d_{31} of the single PSF and the PSF composites are derived, the influences of aspect ratio of the piezoelectric shell, thickness of the electrode layers, and PSF volume fraction, on the effective piezoelectric coefficient d_{31} are investigated.

2. Model and Effective Piezoelectric Coefficients of the Single PSF and the PSF Composites

A PSF and its cross section are shown in figure 1. The proposed model consists of a piezoelectric shell which is polarized along the radial direction (r or x_3 direction), a piezoelectric inactive core fiber which provides the mechanical support to the piezoelectric shell, and inner and outer electrode layers. An electrical potential difference between the inner and outer electrodes gives rise to a radial electrical field which is used to drive the piezoelectric shell, and a corresponding deformation in axial direction (z or x_1 direction) of the PSF is induced by the piezoelectric 31-coupling effect.

The behavior of piezoelectric materials is described by the following constitutive equation:

$$\begin{aligned} \varepsilon_{ij} &= s^{E}_{ijmn}\sigma_{mn} + d_{nij}E_n \\ D_i &= d_{imn}\sigma_{mn} + \kappa^{\sigma}_{in}E_n \end{aligned} \tag{1}$$

where ε_{ij} , σ_{mn} , D_i and E_n are the strain, stress, electric displacement, and electric field, respectively; s_{ijmn}^{E} , d_{nij} and κ_{in}^{σ} are elastic compliance tensor (measured in a constant electric field), piezoelectric field-strain tensor (measured in a constant electric field or at a constant stress), and dielectric tensor (measured at a constant stress), respectively.

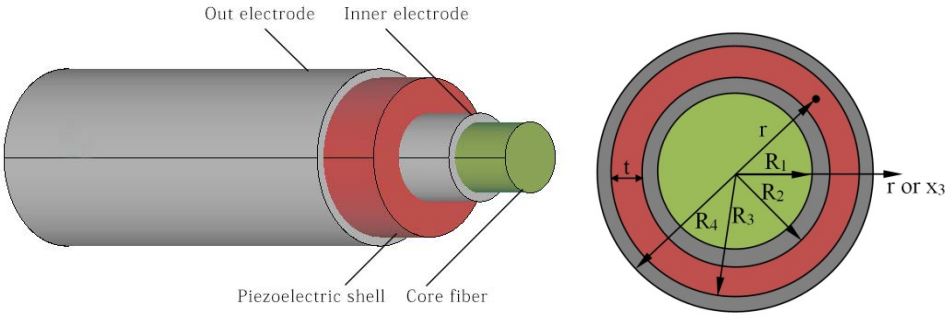

Figure1. Piezoelectric Structural Fiber and Its Cross Section

For the piezoelectric shell, if the material is polarized along the radial direction, it exhibits transversely isotropic behavior in the x_1-x_2 (z - θ) plane, and the constitutive equation (1) can be rewritten as the following matrix form:

$$\begin{pmatrix} \varepsilon_{11} \\ \varepsilon_{22} \\ \varepsilon_{33} \\ \varepsilon_{23} \\ \varepsilon_{31} \\ \varepsilon_{12} \\ D_1 \\ D_2 \\ D_3 \end{pmatrix} = \begin{bmatrix} s_{11}^E & s_{12}^E & s_{13}^E & 0 & 0 & 0 & 0 & 0 & d_{31} \\ s_{12}^E & s_{11}^E & s_{13}^E & 0 & 0 & 0 & 0 & 0 & d_{31} \\ s_{13}^E & s_{13}^E & s_{33}^E & 0 & 0 & 0 & 0 & 0 & d_{33} \\ 0 & 0 & 0 & s_{44}^E & 0 & 0 & 0 & d_{15} & 0 \\ 0 & 0 & 0 & 0 & s_{44}^E & 0 & d_{15} & 0 & 0 \\ 0 & 0 & 0 & 0 & & s_{66}^E & 0 & 0 & 0 \\ 0 & 0 & 0 & 0 & d_{15} & 0 & \kappa_{11}^{\sigma} & 0 & 0 \\ 0 & 0 & 0 & d_{15} & 0 & 0 & 0 & \kappa_{11}^{\sigma} & 0 \\ d_{31} & d_{31} & d_{33} & 0 & 0 & 0 & 0 & 0 & \kappa_{33}^{\sigma} \end{bmatrix} \begin{pmatrix} \sigma_{11} \\ \sigma_{22} \\ \sigma_{33} \\ \sigma_{23} \\ \sigma_{31} \\ \sigma_{12} \\ E_1 \\ E_2 \\ E_3 \end{pmatrix} \tag{2}$$

An electrical potential difference between the inner and outer surfaces of the piezoelectric shell gives rise to an actuating electric field, the expression for the electric field E at a distance r from the geometric center of the piezoelectric shell is given as follows [7]:

$$E(r) = -\frac{V}{r\ln(1-\alpha)} \tag{3}$$

Where t is the wall thickness of the piezoelectric shell, $\alpha = t/R_3$ is the aspect ratio, V is the voltage applied across the piezoelectric shell.

The average electric field in the piezoelectric shell is

$$E_{ave} = \frac{\int_{R_2}^{R_3}\int_0^{2\pi} E(r)rdrd\theta}{\pi(R_3^2 - R_2^2)} = -\frac{E_{tw}}{(1/\alpha - 0.5)\ln(1-\alpha)} \tag{4}$$

Where $E_{tw} = V/t$.

Compared with the length of the PSF, the diameter of the PSF is very small, so the one-dimensional model is usually used to study the 31-coupling effect of the PSF [2], the axial strain in the piezoelectric shell is derived from equation (2) as follows:

$$\varepsilon_{11}(r) = d_{31} E_3(r) \tag{5}$$

The averaged axial strain of the piezoelectric shell is

$$\varepsilon_{11,ave}^{pie} = \frac{\int_{R_2}^{R_3}\int_0^{2\pi} \varepsilon_{11}(r) r dr d\theta}{\pi(R_3^2 - R_2^2)} = \left(-\frac{d_{31}}{(1/\alpha - 0.5)\ln(1-\alpha)} \right) E_{tw} = d_{31,eff}^{pie} E_{tw} \tag{6}$$

Where $d_{31,eff}^{pie}$ is defined as the effective d_{31} of the piezoelectric shell.

Due to the restriction of the electrode layers and the core fiber of the PSF, the piezoelectric shell cannot deform to $\varepsilon_{11,ave}^{pie}$ freely, its practical averaged axial strain is denoted by $\varepsilon_{11,fact}^{pie}$, the averaged axial strains of the electrode layers and the core fiber can also be approximated as $\varepsilon_{11,fact}^{pie}$. Because the resultant axial force on the cross section of the PSF is zero, we have

$$\frac{(\varepsilon_{11,ave}^{pie} - \varepsilon_{11,fact}^{pie})}{s_{11}^{E}} \pi(R_3^2 - R_2^2) = \frac{\varepsilon_{11,fact}^{pie}}{s_{11}^{out}} \pi(R_4^2 - R_3^2) + \frac{\varepsilon_{11,fact}^{pie}}{s_{11}^{in}} \pi(R_2^2 - R_1^2) + \frac{\varepsilon_{11,fact}^{pie}}{s_{11}^{core}} \pi R_1^2 \tag{7}$$

Where s_{11}^{E}, s_{11}^{out}, s_{11}^{in} and s_{11}^{core} are the elastic compliance coefficients of the piezoelectric shell, the outer electrode, inner electrode and the core fiber, respectively.

From equations (6) and (7), $\varepsilon_{11,fact}^{pie}$ is derived as follows:

$$\varepsilon_{11,fact}^{pie} = \left(\frac{\frac{(R_3^2 - R_2^2)}{s_{11}^{E}} d_{31,eff}^{pie}}{\frac{(R_4^2 - R_3^2)}{s_{11}^{out}} + \frac{(R_3^2 - R_2^2)}{s_{11}^{E}} + \frac{(R_2^2 - R_1^2)}{s_{11}^{in}} + \frac{R_1^2}{s_{11}^{core}}} \right) E_{tw} = d_{31,eff}^{PSF} E_{tw} \tag{8}$$

Where $d_{31,eff}^{PSF}$ is defined as the effective d_{31} of the PSF.

To predict the effective d_{31} of the composites embedded with the PSFs, an annular which represents the matrix is attached to the outside of the outer electrode layer of the PSF model, and the area of the annular is determined by the volume fraction of the matrix. Similarly, the effective d_{31} of the PSF composites can then be derived as:

$$d_{11,eff}^{com} = \left(\frac{\frac{(R_3^2 - R_2^2)}{s_{11}^{E}} d_{31,eff}^{pie}}{\frac{(R_5^2 - R_4^2)}{s_{11}^{matrix}} + \frac{(R_4^2 - R_3^2)}{s_{11}^{out}} + \frac{(R_3^2 - R_2^2)}{s_{11}^{E}} + \frac{(R_2^2 - R_1^2)}{s_{11}^{in}} + \frac{R_1^2}{s_{11}^{core}}} \right) E_{tw} = d_{31,eff}^{com} E_{tw} \tag{9}$$

Where $d_{31,eff}^{\text{com}}$ is defined as the effective d_{31} of the PSF composites, R_5 is the outer radius of the matrix annular, s_{11}^{matrix} is the compliance coefficient of the matrix material.

3. Examples

Piezoelectric shells with different aspect ratios have been manufactured through microfabrication by coextrusion technique [9], their diameters are about several hundred micrometers. A PSF consists of a PZT-5A shell, inner and outer wolfram electrode layers, and a glass core fiber is considered. The outer radius of the PZT-5A shell is equal to $300\mu m$, the inner and outer electrode layers have the same thickness. The material properties are listed in Table 1.

Table 1. Material Properties

	PZT-5A	Wolfram	Glass	Epoxy
Elastic compliance coefficient, $\times 10^{-12} m^2 N^{-1}$	$s_{11}^E = 16.4$	2.90	14.3	292.8
Piezoelectric field-strain coefficient, $\times 10^{-12} CN^{-1}$	$d_{31} = -171$	0	0	0

The normalized effective d_{31} of the PSF ($d_{31,eff}^{PSF} / d_{31}$) with respect to the aspect ratio and the normalized effective d_{31} of the PSF composites ($d_{31,eff}^{com} / d_{31}$) with respect to the PSF volume fraction λ for $\alpha = 0.5$ are plotted in figure 2 for several electrode thicknesses (t=0, 1, 3, and $5\mu m$). It is seen from figure 2 that the effective d_{31} of the PSF shows a non-monotonous relationship with the increasing aspect ratio, the maximum value is obtained at approximately $\alpha = 0.74$. The effective d_{31} of the PSF composites shows a sharp increase when λ is small, and then a slow increase is observed with the increasing PSF volume fraction. The electrode layers have significant effects on the effective d_{31} of both the PSF and the PSF composites, the effective d_{31} decreases obviously with the increasing electrode thickness, which indicate that the model without electrode may cause significant errors. It is worth pointing out that the electrode layer leads to the decrease of the effective d_{31}, but a thick electrode is beneficial to prevent the electrode from damage, and improve the mechanical stability of the piezoelectric shell.

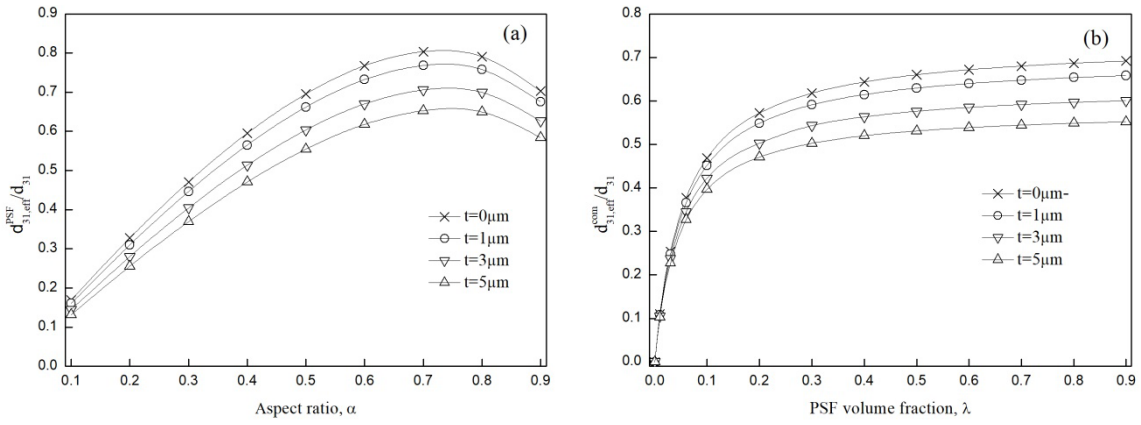

Figure 2. Normalized Effective d_{31} (a) PSF (b) PSF Composites ($\alpha = 0.5$)

4. Conclusions

A refined model is proposed to predict the 31-coupling effect of the PSF and the PSF composites, analytical expressions of the effective piezoelectric coefficient d_{31} of the single PSF and the PSF composites are derived, and the influences of aspect ratio of the piezoelectric shell, thickness of the electrode layer, and PSF volume fraction on the effective d_{31} are demonstrated. The results show that the electrode layers have significant effect on the effective d_{31} of both the PSF and the PSF composites, the model without electrode layers may produce a significant error.

5. References

[1] Bent A A, Hagood N W and Rodgers J P 1995 *J. Intel. Mat. Syst. Str.* **6** 338-49
[2] Niezrecki C, Brei D, Balakrishnan S and Moskalik A 2001 *Shock and Vibration Digest* **33** 269-80
[3] Sodano H A, Park G and Inman D J 2005 *J. Spacecraft Rockets* **42** 370-73
[4] Liu J, Qiu J H, Chang W J, Ji H L and Zhu K J 2010 *Proc. Conf. on Smart Materials, Adaptive Structures and Intelligent Systems* (Philadelphia)
[5] Lin Y and Sodano H A 2008 *Compos. Sci. Technol.* **68** 1911-18
[6] Zhang Q, Wang H and Cross L E 1993 *J. Mater. Sci.* **28** 3962-68
[7] Fernandez J F, Dogan A, Zhang Q M, Tressler J F and Newnham R E 1995 *Sens. Actuator A-Phys.* **51** 183-92
[8] Brei D and Cannon B J 2004 *Compos. Sci. Technol.* **64** 245-61
[9] Cannon B J and Brei D 2000 *Proc. Int. Symposium on Smart Structures and Materials* (San Diego)
[10] Qiu J, Tani J, Yamada N and Takahashi H 2003 *Proc. Int. Symposium on Smart Structure and Materials* (San Diego)
[11] Beckert W, Kreher W, Braue W and Ante M 2001 *J. Eur. Ceram. Soc.* **21** 1455-58
[12] Sebald G, Qiu J, Guyomar Dand Hoshi D 2005 *Japan-Soc. Appl. Phys.* **44** 6136-56
[13] Takagi K, Sato H and Saigo M 2006 *Adv. Compos. Mater.* **15** 403-17
[14] Lin Y and Sodano H A 2009 *Compos. Sci. Technol.* **69** 1825-30.
[15] Dai Q L and Ng K 2012 *Mech. Mater.* **53** 29-46.
[16] Halliday D and Resnick R 1988 *Fundamentals of Physics* (New York: John Wiley & Sons).
[17] Gael S, Abdelmjid B, Jinhao Q, Guiffard B and Guyomar D 2006 *J. Appl. Phys.* **100** 054106-1-6-6